POLITECNICO DI TORINO Repository ISTITUZIONALE

Penny-shaped cracks: A comparison between FFM and CZM

Original

Penny-shaped cracks: A comparison between FFM and CZM / Cornetti, Pietro; Sapora, Alberto. - In: PROCEDIA STRUCTURAL INTEGRITY. - ISSN 2452-3216. - 41:(2022), pp. 505-509. (Intervento presentato al convegno 2nd Mediterranean Conference on Fracture and Structural Integrity tenutosi a Catania, Italy nel 14–16 FEBRUARY) [10.1016/j.prostr.2022.05.057].

Availability: This version is available at: 11583/2966709 since: 2022-06-10T18:39:39Z

Publisher: Elsevier

Published DOI:10.1016/j.prostr.2022.05.057

Terms of use:

This article is made available under terms and conditions as specified in the corresponding bibliographic description in the repository

Publisher copyright

(Article begins on next page)





Available online at www.sciencedirect.com



Procedia Structural Integrity 41 (2022) 505-509

Structural Integrity
Procedia

www.elsevier.com/locate/procedia

2nd Mediterranean Conference on Fracture and Structural Integrity

Penny-shaped cracks: A comparison between FFM and CZM

Pietro Cornetti^{a*}, Alberto Sapora^a

^aDepartment of Structural, Geotechnical and Building Engineering, Politecnico di Torino, Corso Duca degli Abruzzi 24, 10129 Torino, Italy

Abstract

The brittle failure behavior of a solid containing a Penny-shaped crack and subjected to mode I loading conditions is investigated. The analysis is performed in a semi-analytical way by implementing different approaches: the coupled criterion of Finite Fracture Mechanics (FFM) and the Cohesive Zone Model (CZM). Results are compared in terms of the failure stress and the crack advance/process zone.

© 2022 The Authors. Published by Elsevier B.V. This is an open access article under the CC BY-NC-ND license (https://creativecommons.org/licenses/by-nc-nd/4.0) Peer-review under responsibility of the MedFract2Guest Editors.

Keywords: Penny-shaped cracks; mode I; FFM; CZM; failure stress

1. Introduction

Finite Fracture Mechanics (FFM) is a failure criterion proposed for brittle or quasi-brittle materials: it is based on the assumption of a finite crack advance Δ and it involves two parameters, the material tensile strength σ_c and the fracture energy G_c (or the toughness K_{Ic}). Failure load predictions are achieved by coupling the discrete energy with a suitable stress condition. Leguillon set the FFM approach in 2002. Since then, several applications of FFM have been provided and FFM can be now regarded as an effective tool to predict the strength of mechanical components (Sapora et al. 2014, Torabi et al. 2017, Cornetti et al. 2019), allowing fast strength predictions suitable for preliminary sizing of structures.

Although some attempts have been recently done to extend the fracture criterion to 3D cases (Doitrand and Leguillon 2018), most of FFM applications deal with 2D geometries. In this study, the case of a Penny-shaped crack

2452-3216 $\ensuremath{\mathbb{C}}$ 2022 The Authors. Published by Elsevier B.V.

^{*} Corresponding author. Tel.: +39 -011-090- 4901 *E-mail address:* pietro.cornetti@polito.it

This is an open access article under the CC BY-NC-ND license (https://creativecommons.org/licenses/by-nc-nd/4.0)

Peer-review under responsibility of the MedFract2Guest Editors.

^{10.1016/}j.prostr.2022.05.057

subjected to uniform tensile stress is considered (Fig. 1). Although the problem is three-dimensional, the axial symmetry makes the FFM analysis relatively simple, yet interesting for the geometry itself and for possible future 3D extensions. FFM predictions are finally compared with a Dugdale-type Cohesive Crack Model (CCM).

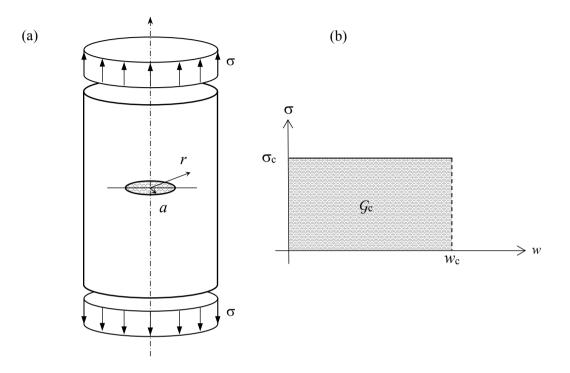


Fig. 1. Penny-shaped crack under uniform remote stress (a); Dugdale-type cohesive law (b).

2. Finite Fracture Mechanics (FFM)

According to the FFM approach (Leguillon 2002), a necessary condition for a finite crack to occur is that the energy available for the crack growth must be higher than the energy required to create the new (annular in the present case) fracture surface. By means of Irwin's relationship we have (Tada et al. 2000):

$$\frac{(1-\nu^2)}{E} \int_{a}^{a+\Delta} K_1^2(a') 2\pi a' da' = \frac{8(1-\nu^2)}{3E} \sigma^2 \Delta \left(3a^2 + 3a\Delta + \Delta^2\right) \ge G_c \pi \left[(a+\Delta)^2 - a^2\right]$$
(1)

Equation (1) can be rewritten as

$$\frac{\sigma}{\sigma_{\rm c}} \ge \sqrt{\frac{3}{8}\pi l_{\rm ch}} \frac{2a + \Delta}{3a^2 + 3a\Delta + \Delta^2}$$
(2)

where $K_{\rm lc} = \sqrt{\frac{G_{\rm c}E}{(1-v^2)}}$ and $l_{\rm ch} = \left(\frac{K_{\rm lc}}{\sigma_{\rm c}}\right)^2$.

The second condition for crack growth is a stress requirement. According to Leguillon's approach, before the crack increment, the stress exceed the material tensile strength on the region where the crack step Δ will take place, i.e. $\sigma_z(r)$

 $\geq \sigma_c$ for $a \leq r \leq a + \Delta$. Since the stress field ahead the crack tip is monotonically decreasing, this condition requires that:

$$\sigma_z \left(r = a + \Delta \right) \ge \sigma_c \tag{3}$$

By using the stress field (Sneddon 1946) one gets:

$$\frac{\sigma}{\sigma_{\rm c}} \ge \frac{\pi}{2} \frac{\sqrt{\Delta(2a+\Delta)}}{a + \sqrt{\Delta(2a+\Delta)} \arccos \frac{a}{a+\Delta}}$$
(4)

According to FFM, both conditions (2) and (4) are necessary for crack growth. Because of their monotonic behavior, the minimum remote failure stress is achieved when both conditions are strictly fulfilled. It means that the actual crack advance is given by the root (Δ_c) of the equation obtained by equating the right hand sides of Eqs. (2) and (4):

$$2\pi\Delta(3a^2 + 3a\Delta + \Delta^2) = 3I_{\rm ch} \left[a + \sqrt{\Delta(2a + \Delta)} \arccos \frac{a}{a + \Delta} \right]^2$$
(5)

The remote failure stress σ_f is finally achieved upon substitution of the root of Eq. (5) into the right hand side either of Eq. (2) or of Eq. (4).

3. Cohesive Zone Model (CZM)

For the Penny-shaped crack, it is also possible to achieve analytical solution by means of a Dugdale-type CCM, i.e. with a rectangular cohesive law, see Fig. 1. According to Dugdale (1960), a plastic annular region of radial size a_p appears ahead the crack tip where stresses are constant and equal to σ_c . The size of this zone is determined by imposing a vanishing SIF at $r = a + a_p$, i.e. at the *fictitious* crack tip:

$$2\sigma_{\infty}\sqrt{\frac{a+a_{\rm p}}{\pi}} - \frac{\sigma_{\rm c}}{\sqrt{\pi(a+a_{\rm p})^2 - a^2}} = 0$$
(6)

Thus (Kelly and Nowell 2000):

$$\frac{a_{\rm p}}{a} = \frac{1}{\sqrt{1 - \left(\sigma_{\infty}/\sigma_{\rm c}\right)^2}} - 1 \tag{7}$$

Crack growth will occur when the opening displacement at the *real* (i.e. at r = a) crack tip reaches the critical value $w_c = G_c/\sigma_c$ (Fig. 1):

$$\frac{8(1-v^2)}{\pi E} \left[\sigma_{\infty} \sqrt{\left(a+a_{\rm p}\right)^2 - a^2} - \sigma_{\rm c} a_{\rm p} \right] = w_{\rm c} \tag{8}$$

Finally, the failure stress and the related process zone size vs. the crack radius a are obtained by inserting Eq. (7) into Eq. (8):

$$\frac{\sigma_{\rm f}}{\sigma_{\rm c}} = \sqrt{1 - \left(1 - \frac{\pi}{8} \frac{l_{\rm ch}}{a}\right)^2} \tag{9}$$

$$a_{\rm p} = \frac{\frac{\pi}{8} l_{\rm ch}}{1 - \frac{\pi}{8} \frac{l_{\rm ch}}{a}}$$
(10)

Equations (9) and (10) hold obviously for crack radii larger than $\pi/8 \times l_{ch}$. Below, a_p is infinite and the failure stress equals the tensile stress.

4. Results and conclusions

FFM and CZM results are plotted in Figs. 2 and 3. As the crack size increases, the finite crack extension decreases from $3/8 \pi \times l_{ch}$ to $1/(2\pi) \times l_{ch}$. For what concerns the process zone, it shows a monotonically decreasing trend with respect to the crack radius as the finite crack extension does. Furthermore, $a_p \rightarrow \pi/8 \times l_{ch}$ as $a \rightarrow \infty$, i.e. a_p tends to Dugdale's plastic zone estimate for large cracks, as expected (Fig. 2).

For what concerns the failure stress (Fig. 3), the agreement between FFM and CCM is excellent: relative differences always keep below 4%. This result validates the present FFM approach (Cornetti and Sapora 2019).

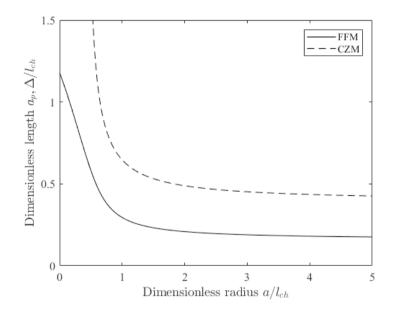


Fig. 2. Finite crack advance according to FFM and process zone size at incipient failure according to CCM versus crack radius.

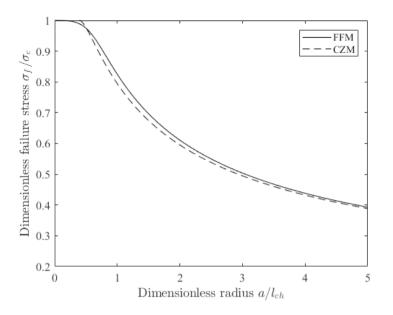


Fig. 3. Failure stress according to FFM and CCM versus crack radius.

The present analysis corroborates the use of FFM as an effective tool to assess the safety of structural components.

References

Cornetti, P., Muñoz-Reja, M., Sapora, A., Carpinteri, A. 2019. Finite fracture mechanics and cohesive crack model: Weight functions vs. cohesive laws. International Journal of Solids and Structures 156-157: 126-136.

Cornetti P., Sapora, A., 2019. Penny-shaped cracks by Finite Fracture Mechanics. International Journal of Fracture 214, 97-104.

Doitrand, A., Leguillon, D., 2018. 3D application of the coupled criterion to crack initiation prediction in epoxy/aluminum specimens under four point bending. International Journal of Solids and Structures 143:175-182.

Dugdale, D.S., 1960. Yielding of steel sheets containing slits. Journal of the Mechanics and Physics of Solids 8:100-108.

Kelly, P.A., Nowell, D., 2000. Three-dimensional cracks with Dugdale-type plastic zones. International Journal of Fracture 106:291-309.

Leguillon, D., 2002. Strength or toughness? A criterion for crack onset at a notch. European Journal of Mechanics A/Solids 21:61-72.

Sapora, A., Cornetti, P., Carpinteri, A., 2014. V-notched elements under mode II loading conditions. Structural Engineering Mechanics 49:499– 508.

Sneddon, I.N., 1946. The distribution of stress in the neighbourhood of a crack in an elastic solid. Proceedings of the Royal Society (London) A187:229-260.

Tada, H., Paris, P., Irwin, G., 2000. The Stress Analysis of Cracks Handbook. ASME Press, New York.

Torabi, A.R., Etesam, S., Sapora, A., Cornetti, P., 2017. Size effects on brittle fracture of Brazilian disk samples containing a circular hole. Engineering Fracture Mechanics 186:496–503.